Bioactive Materials 16 (2022) 293–300

Contents lists available at ScienceDirect

Bioactive Materials

journal homepage: www.keaipublishing.com/en/journals/bioactive-materials

All-small-molecule supramolecular hydrogels assembled from guanosine 5′-monophosphate disodium salt and tobramycin for the treatment of bacterial keratitis

Xuejing Cheng [a,1], Huiyu Chen [b,c,1], Fang Yang [d], Jiaxu Hong [b,***], Yiyun Cheng [a,**], Jingjing Hu [a,*]

[a] Shanghai Key Laboratory of Regulatory Biology, School of Life Sciences, East China Normal University, Shanghai, 200241, China
[b] Department of Ophthalmology, Eye & ENT Hospital, Fudan University, Shanghai, 200031, China
[c] Shanghai Eye Diseases Prevention & Treatment Center, Shanghai Eye Hospital, Shanghai, China
[d] Ophthalmology, Wuhu Hospital affiliated to East China Normal Univesity (The Second Pepole's Hospital of Wuhu), Wuhu, China

ARTICLE INFO

Keywords:
Hydrogel
Supramolecular gel
Antibacterial hydrogel
Aminoglycoside
Bacterial keratitis

ABSTRACT

Bacterial keratitis is the most common corneal infection which may lead to blindness, and seriously threatened the human visual health worldwide. Clinical treatment with antibiotic eye drops formulation usually falls in low bioavailability and poor therapeutic efficiency. Hydrogel has gained much attention as ophthalmic formulation recently due to the prolonged drug retention on ocular surface. In this study, we proposed a type of all-small-molecule supramolecular hydrogel assembled from guanosine-5′-monophosphate disodium salt and tobramycin for the treatment of bacterial keratitis. Guanosine-5′-monophosphate disodium salt assembled into guanosine-quartet nanofibers via hydrogen bonding and π-π stacking, and tobramycin with five primary amine groups further crosslinked the nanofibers bearing multiple phosphate moieties into gel networks via ionic interactions. The supramolecular gel showed shear thinning and thixotropic properties, good biocompatibility, and antibacterial activity. The gel treatment significantly ameliorated *P. aeruginosa* induced bacterial keratitis, and showed higher therapeutic efficacy compared to tobramycin eye drop. This study provides a facile and efficient antibiotic gel formulation for clinical treatment of bacterial keratitis.

1. Introduction

Corneal ulcer is the major cause of visual disability and monocular blindness in lots of the developing countries, ranking second only to cataract [1]. Infectious keratitis caused by bacteria, fungi, virus or parasites is the leading cause of corneal ulcer in clinics, among them, bacterial keratitis showed the highest incidence [2,3]. Lots of daily life incidences including ocular trauma, use of contact lens, ocular surgery and systemic diseases may increase the bacterial infection risk [4]. Once infected, the patients may suffer from acute eye pain, light-sensitivity, decreased visual function, and may cause corneal ulcer perforation if not treated in time, even result in intraocular infection and blindness finally [5,6].

Topical administration of broad-spectrum antibiotics is the main clinical option for treatment of bacterial keratitis. However, conventional ophthalmic administrations (e.g., eye drops and suspensions) are usually suffered from poor bioavailability due to the specific structure and physiological characteristics of eyes (such as low retention time on ocular surface, tear dilution, and nasolacrimal drainage) [4]. Increasing the administration frequency may also bring higher risk of developing bacteria resistance, cumulative systemic side effects and reduced patient compliance [7,8]. To enhance the ocular retention of ophthalmic drugs, various strategies including viscous polymer solutions, adhesive microparticles [5,9–13], and hydrogels [14–16] have been proposed. Among them, hydrogels attracted the most attentions as increasing

Peer review under responsibility of KeAi Communications Co., Ltd.
* Corresponding author.
** Corresponding author.
*** Corresponding author.
E-mail addresses: Jiaxu.hong@fdeent.org (J. Hong), yycheng@mail.ustc.edu.cn (Y. Cheng), jjhu@bio.ecnu.edu.cn (J. Hu).
[1] Xuejing Cheng and Huiyu Chen contributed equally to this work.

https://doi.org/10.1016/j.bioactmat.2021.12.024
Received 25 October 2021; Received in revised form 16 December 2021; Accepted 21 December 2021
Available online 5 January 2022

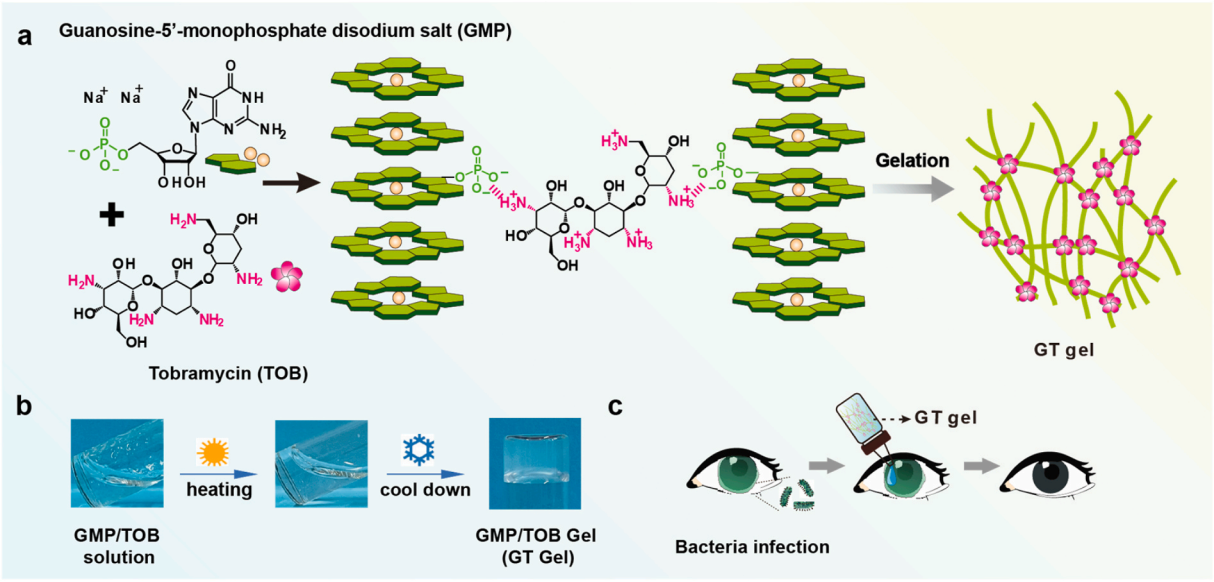

Fig. 1. (a) Illustration of GT Gel formation via electrostatic interactions between GMP-based G-quadruplex and tobramycin. (b) Preparation of GT Gel by a heating and cooling down process. (c) GT Gel for the treatment of bacterial keratitis.

retention time on ocular surface, high moisturizing, and good compatibility [17–25], and the retention time can be extended by almost three times when the formulation was changed from solution to hydrogel [14,22]. Traditional ophthalmic gel is prepared by encapsulation of antibiotic drugs via viscous polymer matrix such as Carbomer [26], or thermo-sensitive polymers such as Pluronic F127 [27]. These non-degradable polymers may cause irritation to the eye tissues [28].

Supramolecular hydrogel assembled from natural small molecules via non-covalent interactions showed great promising in drug delivery systems [29,30]. Their excellent rheological properties including shear thinning and thixotropic property allowed the specific applications including injectable and sprayable formulations [31,32]. These supramolecular gels do not require the pre-synthesis of polymeric scaffolds, and the naturally occurring small-molecule components usually ensured good biocompatibility and biodegradability [21,33,34]. Guanosine-5′-monophosphate, the basic component of RNA, are well-known to form guanosine-quartets (G-quartets) with alkali metal ions via hydrogen bonding and coordination, and further assembled into G-quadruplexes nanofibers through π-π stacking [18,35,36]. Noted that there are multiple negative charged phosphates along the assembled nanofibers [37], we proposed a supramolecular hydrogel fabricated via the electrostatic interactions between guanosine 5′-monophosphate disodium salt (GMP) and tobramycin (TOB), which is the first-line antibacterial drug in the clinical treatment of bacterial keratitis. TOB is a kind of aminoglycoside antibiotic bearing multiple primary amine groups in the structure [28,38–41], the electrostatic interaction between the primary amine groups of TOB and negatively charged phosphates on assembled GMP nanofibers will facilitate the formation of a supramolecular GMP/TOB gel (GT Gel). The possibility of GT Gel in the treatment of *P. aeruginosa* induced bacterial keratitis was investigated (Fig. 1).

2. Materials and methods

2.1. Material

GMP and TOB were purchased from Macklin Biochem. (Shanghai, China). Hydrochloric acid (HCl) was obtained from Sinopharm Chem. (Shanghai, China). Live/dead Baclight™ Bacterial Viability Kits (L13152) was obtained from Thermo Fisher (Carlsbad, USA). Acridine orange (AO)- Ethidium bromide (EB) staining kit and a grinder were obtained from TIANGEN (Beijing, China). 3-(4,5-Dimethylthiazol-2-yl)-2,5-diphenyltetrazolium bromide (MTT) was obtained from Sangon Biotech (Shanghai, China). The Mouse myeloperoxidase (MPO) kit was obtained from Multi Sciences (Hangzhou, China). The RNA extraction kit (EZB-RN4), the Reverse Transcription kit ((A0010CGQ) and Quanti Nova SYBR Green kit (A0012-R2) were obtained from EZBioscience (Beijing, China). *P. aeruginosa* was obtained from ATCC. Hematoxylin-eosin (H&E) staining reagent and TdT-mediated dUTP biotin nick end labeling (TUNEL) assay (In Situ Cell Death Detection Kit) were obtained from Sigma-Aldrich (USA).

2.2. Preparation and characterization of GT Gel

GMP solution was mixed with TOB solution at different molar ratios at pH 5.0, and the mixture was heated at 90 °C for 3 min, and then cooled down to obtain the GT Gel at room temperature. For a typical GT Gel (30 mM GMP, 3 mM TOB), the gel was diluted with deionized water to a final GMP concentration of 50 μM, and characterized by transmission electron microscope (TEM). Generally, 1 μL of the sample was droped onto the copper grid and dried overnight, and captured by a Hitachi microscope (HT7700, Hitachi, Japan) with an acceleration voltage of 100 kV. For atomic force microscope (AFM) characterization, 10 μL of the sample was added onto the silicon chip and naturally dried before measurement (Veeco Dimension 3100, Bruker). For circular dichroism (CD), the sample was loaded in a quartz cell, and the scans were set from 190 to 400 nm (CD, J-815, Jasco International). For rheological measurement, the GT Gel (30 mM GMP, 3 mM TOB) were characterized by a TA rheometer (Discovery HR-3, TA Instrument, USA) at 25 °C, the strain and angular frequency were fixed as 2% and 10 rad/s, respectively. The angular frequency-dependent modulus was measured at a frequency ranged from 0.628 rad/s to 628 rad/s at a sustained strain of 2%. Thixotropic property of GT Gel was studied at a sustained angular frequency of 10 rad/s with an alternative strain of 2% and 100%. The recovery and destruction processes were recorded for 3 cycles.

2.3. Gel degradation and drug release

1 mL GT Gels were immersed in 3 mL phosphate buffered saline (PBS, pH 7.4) at room temperature. The supernatant solutions were collected at scheduled time for further analysis, and the residual gel was weighted. After that, 3 mL fresh PBS solution was added into the gels.

The concentration of TOB in the collected solution was evaluated by a well-established ninhydrin assay. Three repeats were performed for each sample.

2.4. Antibacterial assay

Fresh *P. aeruginosa* was cultured by inoculating a single colony from Luria-Bertani (LB) plate and then added in 5 mL sterile LB medium at 37 °C. The counts of bacteria were assessed by the optical density of the bacterial solution at 600 nm using a microplate reader (Thermo Fisher, Multiskan GO). For the *in vitro* antibacterial assay, 20 μL GT Gels (30 mM GMP, 3 mM TOB) were formed in a 96-well plate. The bacteria solution (10^8 CFU/mL, 100 μL) was added into the wells containing GT Gel, PBS, GMP only, and TOB only, respectively (GMP and TOB concentrations were equal to those in the GT Gel). After incubated at 37 °C for 24 h, the survival bacteria were determined by counting the number of colonies. Three repeats were performed for each sample.

The antibacterial activity of the GT Gel was also evaluated using a Live/dead Baclight™ Bacterial Viability Kit (L13152). After treatment, the bacteria were stained by 30 μM propidium iodide and 6 μM SYTO 9 for 10 min in the dark. Then, 10 μL of the sample was added onto a glass slide and captured by a fluorescence microscope (Olympus HT7700, Japan).

2.5. Biocompatibility assay in vitro

Human corneal epithelial cells (HCEC) kindly provided by Prof. Weiyun Shi (Shandong Eye Institute, Jinan, China) were used to assess the cytotoxicity of GT Gel. The cells were seeded in a 96-well plate and cultured with DMEM containing 10% fetal bovine serum (FBS, Gemini) at 37 °C, and incubated under a humidified 5% CO_2. GMP was dissolved in DMEM at different concentrations, and 100 μL of the solutions were added in each well. Another 24 h later, the cell viability was determined using a standard MTT assay. Five repeats were performed for each sample.

For AO/EB double staining assay, HCEC were cultured in DMEM (10% FBS, 1% streptomycin/penicillin) in 24-well plates at 37 °C. After reaching a cell density of 2×10^5 per well, the culture media were replaced with 400 μL fresh DMEM, and 100 μL of the GT Gel was added into each well. After 24 h, the culture media was removed and the cells were stained with 150 μL AO and EB dye solutions for 5 min in dark. The stained HCEC were observed by a fluorescence microscope (Olympus, Japan).

2.6. Animals

All experimental animal procedures comply with the Association for Research Vision and Ophthalmology Statement about the use of animals. Experiments were approved by the Animal Care and Used Committee of Shanghai Medical College, Fudan University (Animal Ethics Number: IRB-EENT-170607). Wild-type C57 BL/6 mice (8 weeks, male) were obtained from Shanghai SLAC Laboratory Animal Co, Ltd. Mice were raised in a standard environment under 12 h–12 h light-dark cycle.

2.7. Biocompatibility assay in vivo

For *in vivo* biocompatibility assay, eight healthy wild-type C57 BL/6 mice (8 weeks, male) were used to evaluate the biocompatibility of GT Gel *in vivo*. Mice were divided into four groups with 2 mice every group randomly: PBS, GMP, TOB, and GT Gel. 5 μL GT Gel (30 mM GMP, 3 mM TOB), GMP (30 mM), TOB (3 mM), and PBS, respectively were applied on the cornea of each mouse. The treatments were applied once a day with a total of 5 days. After the treatment, the corneas of mice were collected for H&E staining and TUNEL assay, respectively.

Table 1
Primer sequences used for Real-Time PCR.

Primers	Forward (5′-3′)	Reverse(5′-3′)
mGAPDH	CATCACTGCCACCCAGAAGACTG	ATGCCAGTGAGCTTCCCGTTCAG
mIL-6	GTGGCTAAGGACCAAGACCA	TAACGCACTAGGTTTGCCGA
mTNF-α	GCCACCACGCTCTTCTGTCT	TGAGGGTCTGGGCCATAGAAC
mIL-1β	TGCCACCTTTTGACAGTGATG	AAGGTCCACGGGAAAGACAC

2.8. P. aeruginosa induced bacterial keratitis model

The mice were anesthetized via intraperitoneal injection of xylazine (8 mg/kg) and ketamine (80 mg/kg). The whole corneal epithelium was scraped and three superficial stromal incisions were made with a micro scalpel. *P. aeruginosa* (1×10^8 CFU/mL, 5 μL) was then used to infect the wounded cornea. A little pus and edema were observed after the cornea 8 h post infection, indicating the *P. aeruginosa* keratitis model was successfully established. The keratitis mice were randomly divided into four groups (PBS, GMP, TOB, and GT gel) with 5 mice in each group.

2.9. Therapeutic experiments on P. aeruginosa induced bacterial keratitis

5 μL GT Gel (30 mM GMP, 3 mM TOB), GMP (30 mM), TOB (3 mM) and PBS were applied on the infected cornea of each mouse. The treatments were continued once a day for a total of 5 days. For clinical scoring, the severity of *P. aeruginosa* induced bacterial keratitis was examined daily up to 5 days post infection with a slit lamp microscope (Topcon, Tokyo, Japan) and scored as follows: a grade of 0–4 was individually assigned to criteria including area of opacity, density of opacity, and surface regularity. Briefly, a transparent and clarified cornea was assessed with 0 in each criterion. The total of clinical score ranged from 0 to 12.

For bacterial load determination, the cornea tissues were excised after the mice were sacrificed and placed in 200 μL PBS. The tissues were then homogenized with a grinder. 100 μL of the original homogenate was confected into serial log dilutions with PBS for bacterial loading assessment. 50 μL of serial log dilutions were inoculated onto isolation agar plates in triplicates for 24 h at 37 °C to count *P. aeruginosa* colonies. The remaining 100 μL homogenate was centrifuged to obtain supernatant for myeloperoxidase (MPO) assay using a mouse MPO kit as the manufacturer's instructions.

For quantitative real-time PCR, the total RNA of mice corneas was extracted using the RNA extraction kit. The first strand cDNA was reverse transcribed with the Reverse Transcription kit. Quantitative real-time PCR was examined using primer sequences (Table 1) and QuantiNova SYBR Green kit following the manufacturer's instructions. Data were processed using the comparative Ct method. GAPDH was used as an internal control.

For TUNEL assay, the frozen mice cornea sections were fixed in 4% paraformaldehyde at 4 °C for 25 min, followed by PBS washing for three times. After permeated in 0.2% Triton X-100 for 15min at room temperature, the tissues were stained with pre-mixed terminal deoxynucleotidyl transferase solution containing label solution (TMR-dUTP) in the dark at 37 °C for 1 h. The nuclei were then stained with DAPI. Images were observed and captured using a fluorescence microscope (TSE SPE; Leica Microsystems, Wetzlar, Germany). For H&E staining, the harvested tissues were fixed in formalin, followed by paraffin embedding, sectioned, and H&E staining to evaluate the level of inflammatory infiltrates.

3. Results and discussion

Transparent GT hydrogels were formed when the mixture of GMP and TOB solutions at proper GMP/TOB ratios were heated and cooled down to room temperature. According to the phase diagram in Fig. 2a, GMP at 30 mM formed hydrogels with TOB at a wide range of TOB

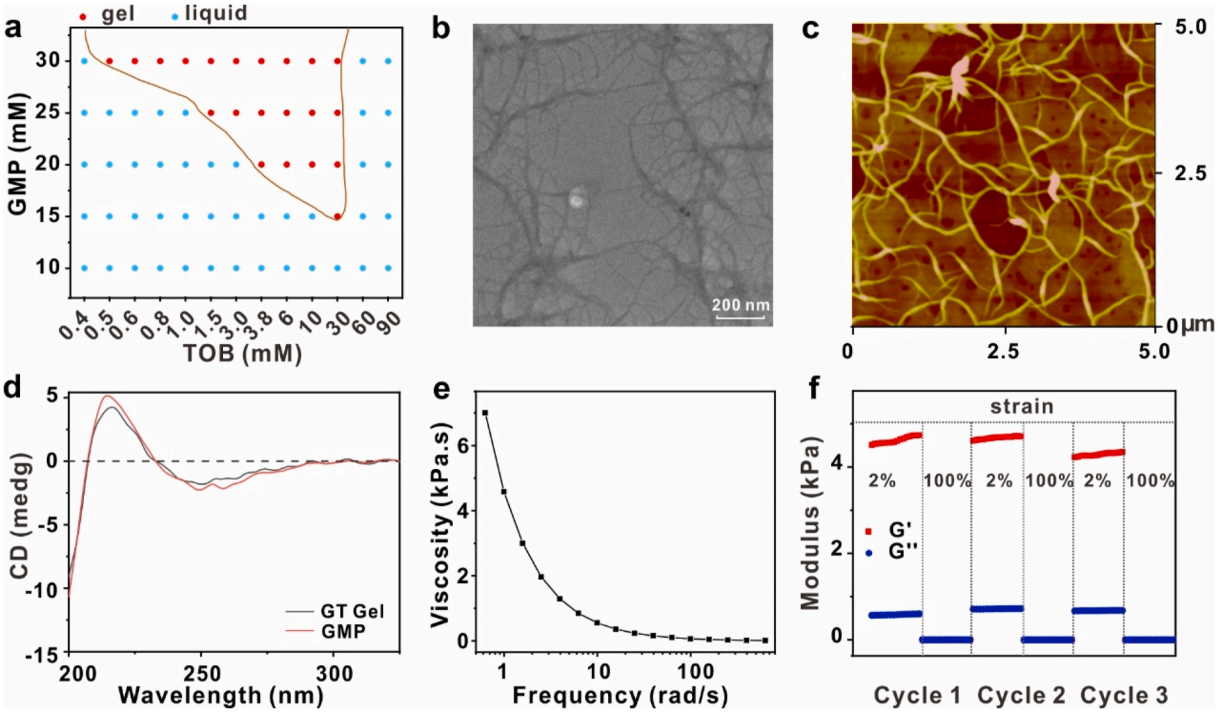

Fig. 2. (a) Phase diagram of GMP/TOB mixtures at different GMP and TOB concentrations. (b) TEM image of GT Gel (30 mM GMP and 3 mM TOB). Scale bar, 200 nm. (c) AFM image of the GT Gel (30 mM GMP and 3 mM TOB). (d) CD spectra of the GT Gel (30 mM GMP and 3 mM TOB). 30 mM GMP is tested as a control. (e) Shear-thinning behavior of GT Gel (30 mM GMP and 3 mM TOB). The angular frequency was swept from 0.628 to 628 rad/s at a constant strain of 2%. (f) The thixotropic properties of GT Gel (30 mM GMP and 3 mM TOB). Recovery and breaking of the hydrogel were carried out for three recycles at a constant angular frequency of 10 rad/s with an alternative strain of 2 and 100%, respectively.

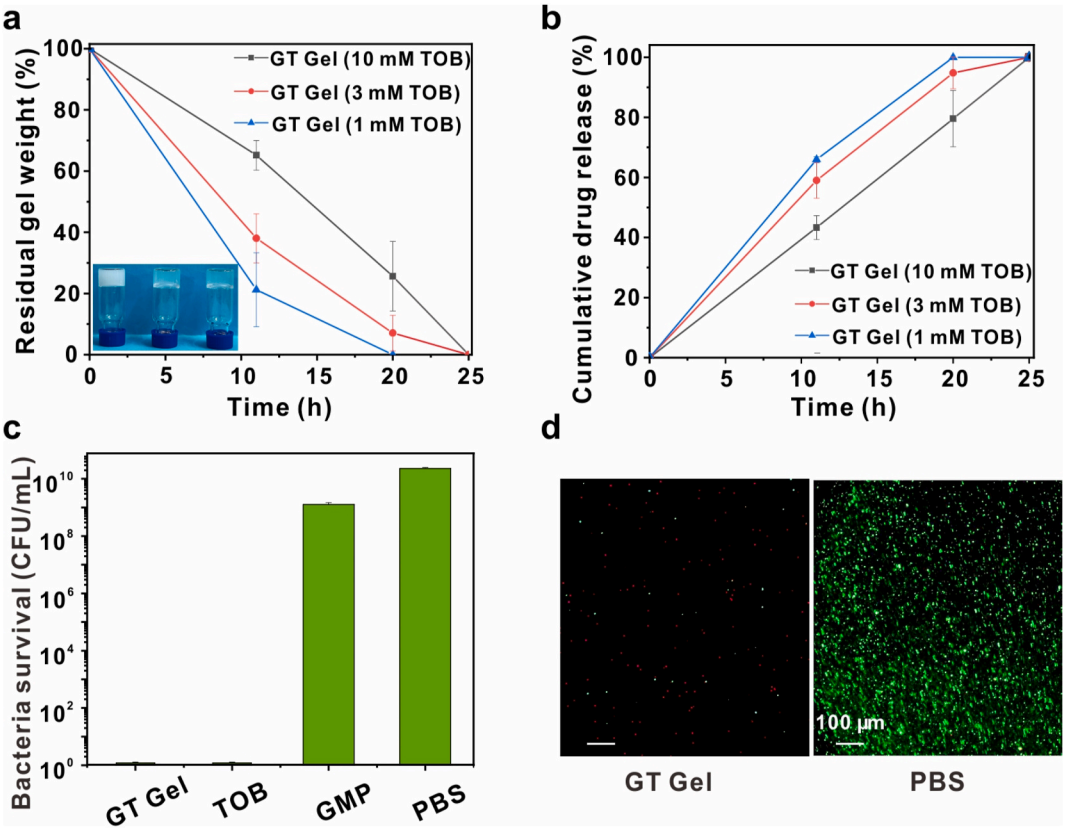

Fig. 3. The residual gel weight (a) and the cumulative TOB release (b) of the GT Gels (30 mM GMP, 1–10 mM TOB). (c) *In vitro* antibacterial activity of GT Gel, TOB, GMP against *P. aeruginosa*. (d) Live/dead staining images of *P. aeruginosa* treated with GT Gel and PBS. Scale, 100 μm.

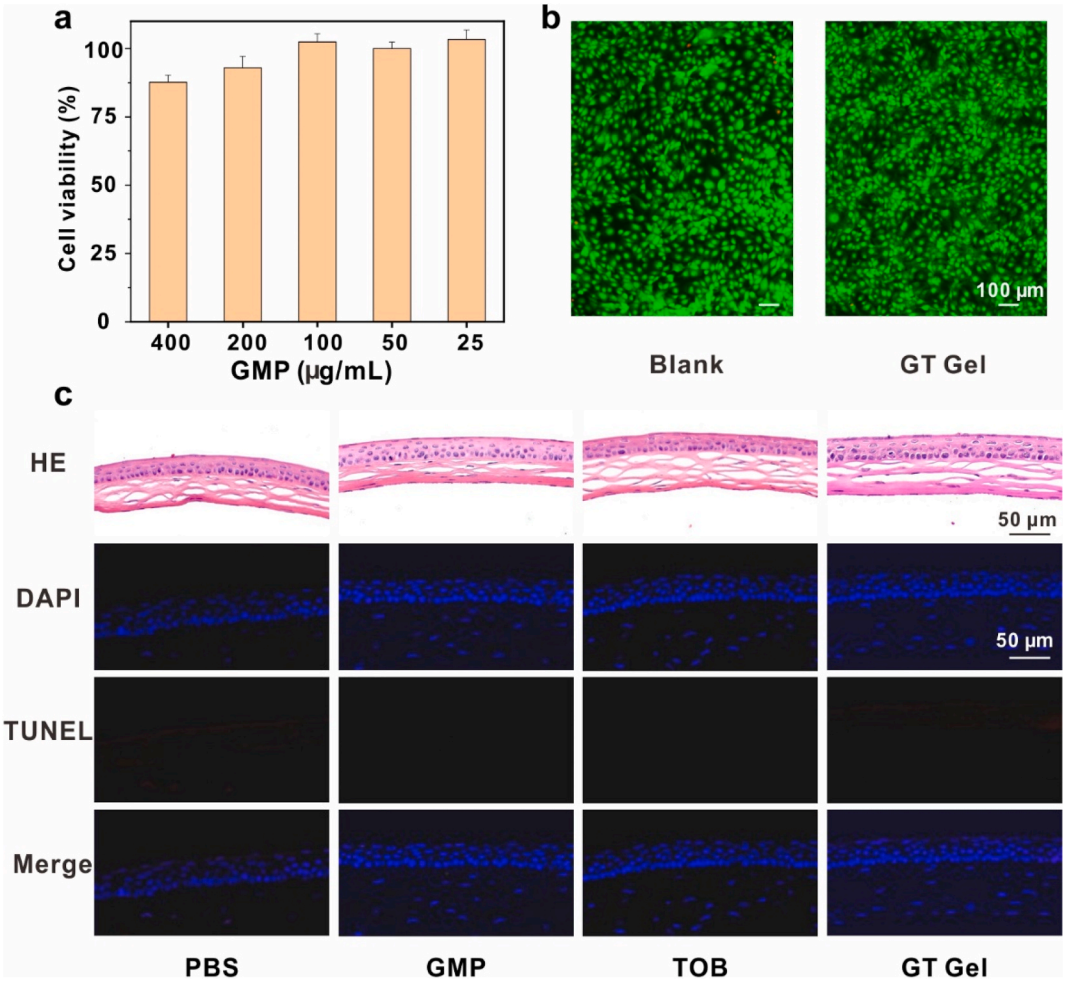

Fig. 4. (a) Cytotoxicity of GMP on HCEC tested by MTT assay. (b) AO/EB staining of HCEC treated with GT Gel. Scale, 100 μm. (c) The H&E and TUNEL staining images of the cornea treated with PBS, GMP, TOB and GT Gel, respectively. Scale, 50 μm.

concentrations (0.5–30 mM). When decreasing the GMP concentrations, higher TOB concentrations are required to prepare the gel. This is because TOB molecule bearing five primary amine groups acted as a crosslinking ligand between the negatively charged GMP nanofibers via electrostatic interactions in the gel system. Higher concentrations of both GMP and TOB indicate more efficient crosslinking density in the gel. It is worth noting that GMP itself failed to form hydrogels at the investigated concentrations (10–30 mM). We further characterized a typical GT hydrogel consisting of 30 mM GMP and 3 mM TOB. Both TEM and AFM results revealed that crosslinked nanofibrous structures are observed in the gel network (Fig. 2b–c), which is due to the supramolecular assembly of GMP molecules into nanofibers via hydrogel bonding and π-π stacking, and the crosslinking of GMP fibers by TOB via ionic interactions. CD spectrum suggested that the presence of TOB does not change the original structure of assembled GMP nanofibers (Fig. 2d), which performed a head-to-tail signature of the guanosine quartets [42]. Moreover, the rheological results suggested that the GT Gel is shear thinning and thixotropic (Fig. 2e–f), which allow the gel to become less viscous and spread along the ocular surface when encountering shear forces, such as blinking.

We further investigated the gel degradation and drug release of GT Gels consisting of 30 mM GMP and 1–10 mM TOB. As shown in Fig. 3a, the GT Gels were gradually degraded within 25 h, and a slower gel degradation was observed for GT Gels with higher TOB concentrations. Similarly, GT Gels with higher TOB concentrations showed slower TOB release rate (Fig. 3b). This is due to higher crosslinking density in the gel network at higher TOB concentrations. With increasing the TOB concentration, the gel appearance changed from transparent (3 mM TOB) to non-transparent (10 mM TOB). Considering that transparency is an important parameter for ophthalmic gels, GT Gel containing 30 mM GMP and 3 mM TOB was used for later studies. The GT Gel maintained the high antibacterial activity of TOB against *P. aeruginosa* (Fig. 3c and d). The biocompatibility of GT Gel *in vitro* and *in vivo* was further evaluated. As shown in Fig. 4a, GMP at concentrations up to 400 μg/mL showed minimal toxicity on HCEC. Besides GMP, GT Gels showed low toxicity on HCEC as revealed by AO/EB staining assay (Fig. 4b). To evaluate the biocompatibility of GMP and GT Gel *in vivo*, the samples were administrated on the cornea of healthy mouse every day with a total of 5 days. After treatment, no obvious inflammation and apoptosis in the cornea tissues were observed according to the H&E staining and TUNEL assay (Fig. 4c).

We finally evaluated the therapeutic efficacy of GT Gels on *P. aeruginosa* induced bacterial keratitis (Fig. 5a). *P. aeruginosa* is the most common devastating corneal pathogen, and it may result in severe ulcerative keratitis and worse visual outcome. As shown in Fig. 5b, nearly all the infected mice treated with PBS and GMP were observed with opaque cornea at day 3 after infection, and obvious neovascularization as well as melting ulceration at day 5. The severe symptoms of keratitis were significantly alleviated at day 1 and day 3 when the mice were treated with TOB eye drop and GT Gel. However, obvious opacity was observed on the cornea of mice treated with free TOB eye drop at day 5, while GT Gel treated cornea still showed transparent appearance. The clinical scores of GT Gel treated mice were also lower than those of mice treated with PBS, GMP and TOB at day 5

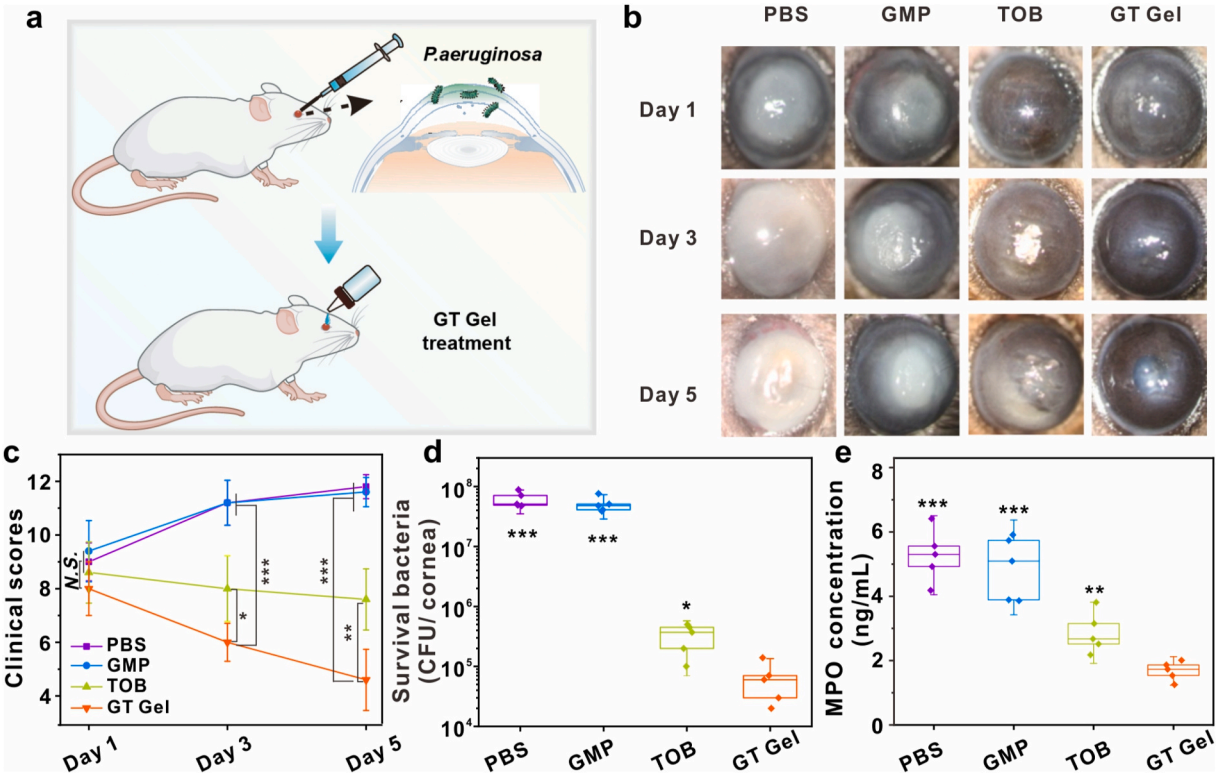

Fig. 5. (a) GT Gel for the treatment of *P. aeruginosa* induced keratitis. (b) Representative appearance of infected corneas at scheduled times after treatment. (c) The severity of *P. aeruginosa* induced bacterial keratitis evaluated with clinical scores ranging from 0 to 12. The survival bacteria colonies (d) and MPO levels (e) in the cornea tissues after treatment (Data represented mean ± SD, n = 5. $^{*}p < 0.05$, $^{**}p < 0.01$, $^{***}p < 0.001$ analyzed by unpaired Student's *t*-test, a comparison between GT gel and the other groups).

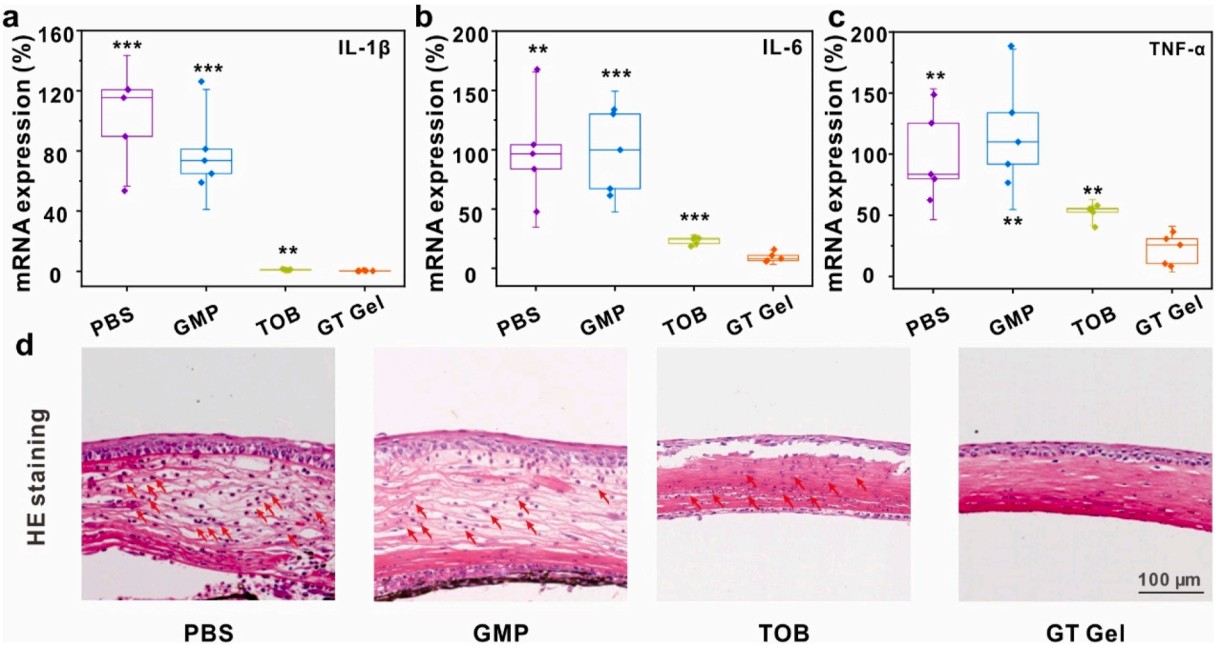

Fig. 6. RT-PCR analysis of proinflammatory cytokines including IL-1β, IL-6 and TNF-α in cornea of mice treating with PBS, GMP, TOB and GT Gel (a–c). Representative H&E staining images in cornea of mice treated with PBS, GMP; TOB and GT Gel. The red arrows indicate inflammatory cell infiltration (d). Scale, 100 μm. Data represented mean ± SD, n = 5. $^{*}p < 0.05$, $^{**}p < 0.01$, $^{***}p < 0.001$ analyzed by unpaired Student's *t*-test, a comparison between GT gel and the other groups.

(Fig. 5c). Besides, the colony forming units of *P. aeruginosa* in GT Gel treated cornea was three orders of magnitudes lower than those in PBS- and GMP- treated ones, and one order of magnitude lower than that in the TOB eye drop treated ones (Fig. 5d). In addition, the GT Gel treated cornea showed lower MPO levels than the control groups, indicating reduced neutrophil infiltration in the infected cornea after GT Gel treatment (Fig. 5e). The higher therapeutic efficacy of GT Gel than TOB eye drop should be attributed to sustained TOB release from the gel on

ocular surface.

It is known that *P. aeruginosa* may initiate the host innate response by recruiting macrophages and other immune cells to the infection site, and the immune cells could produce pro-inflammatory cytokines such as interleukin-6 (IL-6), IL-1β and tumor necrosis factor-α (TNF-α) to eliminate the bacteria. However, overexpression of inflammatory cytokines may trigger inflammatory cascade which could lead to tissue melting and decreased cornea transparency. We also investigated the level of innate immune response genes and inflammatory infiltration in the treated cornea. As shown in Fig. 6a–c, the pro-inflammatory cytokines including IL-1β, IL-6 and TNF-α were significantly suppressed after GT Gel treatment. The inflammatory infiltration and corneal collagenous fiber edema were also significantly reduced as revealed by H&E staining results (Fig. 6d). All these results suggest that the GT Gel is more efficient than TOB eye drop with equal drug concentration, which is an effective and biocompatible antibiotic formulation for the treatment of bacterial keratitis.

4. Conclusions

In summary, we proposed a facile strategy to prepare supramolecular gels consisting of all-small-molecule natural building blocks. The hydrogel is formed by ionic interactions between antibiotic drug TOB and GMP-based G-quartet nanofibers. The prepared gel showed good transparency, thixotropic property, biocompatibility, sustained drug release, and therapeutic efficacy on the *P. aeruginosa* induced bacterial keratitis. The results provide a promising gel candidate for clinical treatment of bacterial keratitis.

CRediT authorship contribution statement

Xuejing Cheng: Methodology, Formal analysis, Data curation, Writing – original draft. **Huiyu Chen:** Methodology, Formal analysis, Data curation, Writing – original draft. **Fang Yang:** Methodology, Formal analysis, Writing – review & editing. **Jiaxu Hong:** Resources, Writing – review & editing, Supervision. **Yiyun Cheng:** Conceptualization, Writing – review & editing, Supervision. **Jingjing Hu:** Conceptualization, Writing – review & editing, Supervision.

Declaration of competing interest

The authors declare that they have no known competing financial interests or personal relationships that could have appeared to influence the work reported in this paper.

Acknowledgements

We greatly appreciate the grants from the Natural Science Foundation of Shanghai (19ZR1415600), the National Natural Science Foundation of China (81970766 and 82171102), the Program for Professor of Special Appointment (Estern Scholar) at Shanghai Institutions of Higher Learning, the Shanghai Innovation Development Program (2020-RGZN-02033), the Shanghai Key Clinical Research Program (SHDC2020CR3052B) and the Fundamental Research Funds for the Central Universities.

References

[1] J.P. Whitcher, M. Srinivasan, M.P. Upadhyay, Corneal blindness: a global perspective, Bull. World Health Organ. 79 (3) (2001) 214–221.
[2] P.A. Thomas, P. Geraldine, Infectious keratitis, Curr. Opin. Infect. Dis. 20 (2) (2007) 129–141.
[3] S. Egrilmez, Ş. Yildirim-Theveny, Treatment-resistant bacterial keratitis: challenges and solutions, Clin. Ophthalmol. 14 (2020) 287–297.
[4] L. Keay, K. Edwards, T. Naduvilath, H.R. Taylor, G.R. Snibson, K. Forde, F. Stapleton, Microbial keratitis predisposing factors and morbidity, Ophthalmology 113 (1) (2006) 109–116.
[5] H.J. Jian, R.S. Wu, T.Y. Lin, Y.J. Li, H.J. Lin, S.G. Harroun, J.Y. Lai, C.C. Huang, Super-cationic carbon quantum dots synthesized from spermidine as an eye drop formulation for topical treatment of bacterial keratitis, ACS Nano 11 (7) (2017) 6703–6716.
[6] D. Rachwalik, U. Pleyer, Bacterial keratitis, Klin. Monbl. Augenheilkd. 232 (6) (2015) 738–744.
[7] L.R. Hoffman, D.A. D'Argenio, M.J. MacCoss, Z. Zhang, R.A. Jones, S.I. Miller, Aminoglycoside antibiotics induce bacterial biofilm formation, Nature 436 (7054) (2005) 1171–1175.
[8] X. Yuan, D.C. Marcano, C.S. Shin, X. Hua, L.C. Isenhart, S.C. Pflugfelder, G. Acharya, Ocular drug delivery nanowafer with enhanced therapeutic efficacy, ACS Nano 9 (2) (2015) 1749–1758.
[9] D. Ding, B. Kundukad, A. Somasundar, S. Vijayan, S.A. Khan, P.S. Doyle, Design of mucoadhesive PLGA microparticles for ocular drug delivery, ACS Appl. Bio. Mater. 1 (3) (2018) 561–571.
[10] H. Li, X. Wang, X. Zhao, G. Li, F. Pei, H. Zhang, Y.A.-O. Tan, F. Chen, Vacancy-induced antibacterial activity of XS(2-) (y) quantum dots against drug-resistant bacteria for treatment of bacterial keratitis, Small 16 (42) (2020), 2004677.
[11] X. Zhou, J. Lv, G. Li, T. Qian, H. Jiang, J. Xu, Y. Cheng, J. Hong, Rescue the retina after the ischemic injury by polymer-mediated intracellular superoxide dismutase delivery, Biomaterials 268 (2021), 120600.
[12] A. Yu, H. Shi, H. Liu, Z. Bao, M. Dai, D. Lin, D. Lin, X. Xu, X. Li, Y. Wang, Mucoadhesive dexamethasone-glycol chitosan nanoparticles for ophthalmic drug delivery, Int. J. Pharm. 575 (2020), 118943.
[13] H. Chen, J. Yang, L. Sun, H. Zhang, Y. Guo, J. Qu, W. Jiang, W. Chen, J. Ji, Y. W. Yang, B. Wang, Synergistic chemotherapy and photodynamic therapy of endophthalmitis mediated by zeolitic imidazolate framework-based drug delivery systems, Small 15 (47) (2019), 1903880.
[14] Z. Zhang, Z. He, R. Liang, Y. Ma, W. Huang, R. Jiang, S. Shi, H. Chen, X. Li, Fabrication of a micellar supramolecular hydrogel for ocular drug delivery, Biomacromolecules 17 (3) (2016) 798–807.
[15] N. Bayat, Y. Zhang, P. Falabella, R. Menefee, J.J. Whalen 3rd, M.S. Humayun, M. E. Thompson, A reversible thermoresponsive sealant for temporary closure of ocular trauma, Sci. Transl. Med. 9 (419) (2017) 3879.
[16] E. Shirzaei Sani, A. Kheirkhah, D. Rana, Z. Sun, W. Foulsham, A. Sheikhi, A. Khademhosseini, R. Dana, N. Annabi, Sutureless repair of corneal injuries using naturally derived bioadhesive hydrogels, Sci. Adv. 5 (3) (2019) 1281.
[17] A. Harada, Y. Takashima, M. Nakahata, Supramolecular polymeric materials via cyclodextrin-guest interactions, Acc. Chem. Res. 47 (7) (2014) 2128–2140.
[18] G.M. Peters, J.T. Davis, Supramolecular gels made from nucleobase, nucleoside and nucleotide analogs, Chem. Soc. Rev. 45 (11) (2016) 3188–3206.
[19] S. Khosravimelal, M. Mobaraki, S. Eftekhari, M. Ahearne, A.M. Seifalian, M. Gholipourmalekabadi, Hydrogels as emerging materials for cornea wound healing, Small 17 (30) (2021), 2006335.
[20] C. Wang, C. Liu, Q. Wei, L. Yang, P. Yang, Y. Li, Y. Cheng, S,S-Tetrazine-based hydrogels with visible light cleavable properties for on-demand anticancer drug delivery, Research 2020 (2020) 1–11.
[21] T. Dai, C. Wang, Y. Wang, W. Xu, J. Hu, Y. Cheng, A nanocomposite hydrogel with potent and broad-spectrum antibacterial activity, ACS Appl. Mater. Interfaces 10 (17) (2018) 15163–15173.
[22] Z. Zhang, J. Yu, Y. Zhou, R. Zhang, Q. Song, L. Lei, X. Li, Supramolecular nanofibers of dexamethasone derivatives to form hydrogel for topical ocular drug delivery, Colloids Surf. B Biointerfaces 164 (2018) 436–443.
[23] D. Lin, L. Lei, S. Shi, X. Li, Stimulus-Responsive hydrogel for ophthalmic drug delivery, Macromol. Biosci. 19 (6) (2019), 1900001.
[24] X. Ding, S. Duan, X. Ding, R. Liu, F.-J. Xu, Versatile antibacterial materials: an emerging arsenal for combatting bacterial pathogens, Adv. Funct. Mater. 28 (40) (2018), 1802140.
[25] S.S. Liow, Q. Dou, D. Kai, A.A. Karim, K. Zhang, F. Xu, X.J. Loh, Thermogels: in Situ gelling biomaterial, ACS Biomater. Sci. Eng. 2 (3) (2016) 295–316.
[26] T.Y. Chou, B.Y. Hong, Ganciclovir ophthalmic gel 0.15% for the treatment of acute herpetic keratitis: background, effectiveness, tolerability, safety, and future applications, Therapeut. Clin. Risk Manag. 10 (2014) 665–681.
[27] H. Yang, P. Tyagi, R.S. Kadam, C.A. Holden, U.B. Kompella, Hybrid dendrimer hydrogel/PLGA nanoparticle platform sustains drug delivery for one week and antiglaucoma effects for four days following one-time topical administration, ACS Nano 6 (9) (2012) 7595–7606.
[28] J. Hu, Y. Quan, Y. Lai, Z. Zheng, Z. Hu, X. Wang, T. Dai, Q. Zhang, Y. Cheng, A smart aminoglycoside hydrogel with tunable gel degradation, on-demand drug release, and high antibacterial activity, J. Contr. Release 247 (2017) 145–152.
[29] S. Bernhard, M.W. Tibbitt, Supramolecular engineering of hydrogels for drug delivery, Adv. Drug Deliv. Rev. 171 (2021) 240–256.
[30] X. Du, J. Zhou, J. Shi, B. Xu, Supramolecular hydrogelators and hydrogels: from soft matter to molecular biomaterials, Chem. Rev. 115 (24) (2015), 13165-13307.
[31] S. Seiffert, J. Sprakel, Physical chemistry of supramolecular polymer networks, Chem. Soc. Rev. 41 (2) (2012) 909–930.
[32] X. Ma, Y. Zhao, Biomedical applications of supramolecular systems based on host-guest interactions, Chem. Rev. 115 (15) (2015) 7794–7839.
[33] M. Li, H. Wang, J. Hu, J. Hu, S. Zhang, Z. Yang, Y. Li, Y. Cheng, Smart hydrogels with antibacterial properties built from all natural building blocks, Chem. Mater. 31 (18) (2019) 7678–7685.
[34] J. Hu, Q. Hu, X. He, C. Liu, Y. Kong, Y. Cheng, Y. Zhang, Stimuli-Responsive hydrogels with antibacterial activity assembled from guanosine, aminoglycoside, and a bifunctional anchor, Adv. Healthc. Mater. 9 (2) (2020), 1901329.
[35] J.T. Davis, G.P. Spada, Supramolecular architectures generated by self-assembly of guanosine derivatives, Chem. Soc. Rev. 36 (2) (2007) 296–313.

[36] J.T. Davis, G-quartets 40 years later: from 5'-GMP to molecular biology and supramolecular chemistry, Angew Chem. Int. Ed. Engl. 43 (6) (2004) 668–698.
[37] R. Belda, E. García-España, G.A. Morris, J.W. Steed, J.A. Aguilar, Guanosine-5'-Monophosphate polyamine hybrid hydrogels: enhanced gel strength probed by z-spectroscopy, Chemistry 23 (32) (2017) 7755–7760.
[38] J. Hu, Z. Zheng, C. Liu, Q. Hu, X. Cai, J. Xiao, Y. Cheng, A pH-responsive hydrogel with potent antibacterial activity against both aerobic and anaerobic pathogens, Biomater. Sci. 7 (2) (2019) 581–584.
[39] H. Wang, Y. Cheng, All-small-molecule dynamic covalent hydrogels with multistimuli responsiveness, Mater. Chem. Front. 3 (3) (2019) 472–475.
[40] J. Hu, L. Yang, X. Cheng, Y. Li, Y. Cheng, Aminoglycoside-based biomaterials: from material design to antibacterial and gene delivery applications, Adv. Funct. Mater. 31 (36) (2021), 2103718.
[41] J. Hu, C. Zhang, L. Zhou, Q. Hu, Y. Kong, D. Song, Y. Cheng, Y. Zhang, A smart hydrogel for on-demand delivery of antibiotics and efficient eradication of biofilms, Sci. Chin. Mater. 64 (4) (2020) 1035–1046.
[42] A. Ghosh, B. Parasar, T. Bhattacharyya, J. Dash, Chiral carbon dots derived from guanosine 5'-monophosphate form supramolecular hydrogels, Chem. Commun. 52 (74) (2016) 11159–11162.